

Towards General and Efficient Active Learning

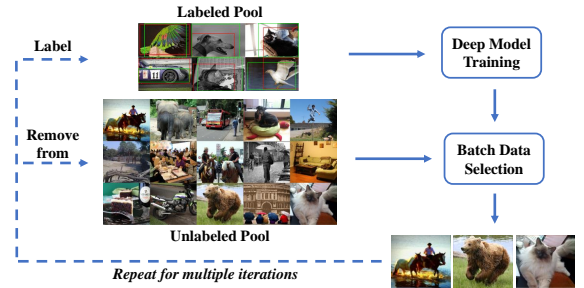
Yichen Xie, Masayoshi Tomizuka, Wei Zhan*
 University of California, Berkeley
 {yichen.xie, tomizuka, wzhan}@berkeley.edu

Abstract

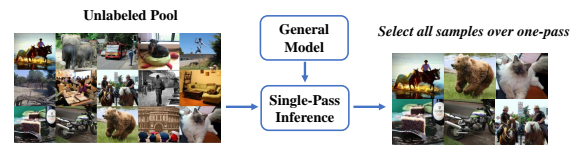
Active learning aims to select the most informative samples to exploit limited annotation budgets. Most existing work follows a cumbersome pipeline by repeating the time-consuming model training and batch data selection multiple times on each dataset separately. We challenge this status quo by proposing a novel general and efficient active learning (GEAL) method in this paper. Utilizing a publicly available model pre-trained on a large dataset, our method can conduct data selection processes on different datasets with a single-pass inference of the same model. To capture the subtle local information inside images, we propose knowledge clusters that are easily extracted from the intermediate features of the pre-trained network. Instead of the troublesome batch selection strategy, all data samples are selected in one go by performing K-Center-Greedy in the fine-grained knowledge cluster level. The entire procedure only requires single-pass model inference without training or supervision, making our method notably superior to prior arts in terms of time complexity by up to hundreds of times. Extensive experiments widely demonstrate the promising performance of our method on object detection, semantic segmentation, depth estimation, and image classification. Our code will be made publicly available in https://github.com/yichen928/GEAL_active_learning.

1. Introduction

Deep Neural Network (DNN) models have achieved exciting performance in various tasks. Such success is supported by abundant training samples and labels. Despite the availability of some large annotated datasets [13, 48], current models are still far from saturation [38] with respect to the data amount. Unfortunately, labeling a dataset tends to be time-consuming and expensive, especially for dense supervision tasks such as object detection and semantic segmentation, where experts spend up to 90 minutes per image [35]. As such, how to exploit the limited annotation



(a) **Traditional Pipeline of Active Learning:** Model training and batch data selection repeat multiple times on each dataset.



(b) **Our Pipeline:** Samples are selected with *one-pass* model inference on each dataset.

Figure 1. **Traditional Pipeline** v.s. **Our Proposed Pipeline of Active Learning**

budget serves as a long-standing problem for the further development of computer vision and machine learning.

As a potential solution, active learning methods [47, 50] attempt to find the most suitable samples for annotation which can best boost the training of task models. In the area of deep learning, almost all existing active learning methods rely on DNNs to process the data samples. The costly and time-consuming model training process prevents them from being easily and widely used. To be specific, most approaches work in a traditional *batch selection* pipeline [49], as shown in Fig. 1a. A deep model is firstly trained on a randomly sampled small subset, and it is then used to choose images with a certain batch size. These selected images are annotated and put into the labeled pool, and the model is re-trained or fine-tuned on all the labeled samples again. These steps repeat for multiple iterations on a large dataset, and the whole pipeline should start from scratch when we work on another dataset. In many cases, it even requires *several days* to select enough samples from a medium-size

*Correspondence

dataset (*e.g.* PASCAL VOC [17] in Tab. 1).

In this paper, we challenge this *status quo* by designing a novel active learning pipeline (Fig. 1b). First of all, we consider the following three principles of our design.

Generality Deep models are necessary for feature extraction in the active learning pipeline. It is desired that a *general* pre-trained model can work over multiple datasets so that the model does not require training on each dataset separately.

Efficiency The traditional *batch selection* setting (Fig. 1a) is known to be time-consuming due to the iterative batch data selection and model training on each dataset. Ideally, it is expected to be replaced with a *single-pass* model inference for feature extraction.

Non-supervision Annotators cannot always respond in time, and the entire active learning progress may be delayed by the request of labels. This problem exists in many prior work [1, 49, 61]. To this end, it is preferred that annotations are not required in the pipeline of active learning.

In view of the above principles, we propose a novel general and efficient active learning (GEAL) method. To the best of our knowledge, it is the first method satisfying all the above principles simultaneously.

The proposed method uses a publicly available pre-trained model to extract features from images. Thanks to the unsupervised pre-training [4] on a large scale dataset [13], the model bias is small, and we can apply the *same* pre-trained model to different datasets. The selected samples are also network agnostic, *i.e.* the architectures of pre-trained model and downstream task models may be totally different.

In pursuit of *efficiency*, our method gets rid of the repetitive model training in the traditional pipeline. Instead, we directly perform *K-Center-Greedy* algorithm *w.r.t.* the *knowledge clusters* coming from the intermediate features of each image extracted by the pre-trained model. The whole data selection process for each dataset is conducted with only a *single-pass* inference of the pre-trained model. It successfully reduces the time complexity by *hundreds of times* in comparison with previous work following the traditional pipeline.

It is also worth mentioning that samples are selected based on the distance between extracted intermediate features. As a result, annotations are not required in the entire active learning pipeline. That is to say, our method is indeed *unsupervised*, which relieves the troubles of assigning responsive annotators.

We conduct extensive experiments over different tasks, datasets, and networks. Results demonstrate notable superiority of our algorithm to random selection and other general

Table 1. **Generality and Efficiency of Active Learning Methods:** *Train* refers to the necessity of training a deep model separately for each dataset. *Batch* shows whether the method repeats the data selection in batch multiple times. *Sup.* denotes whether it requests ground-truth label in the data selection process. *Time* estimates the approximate time to select 8000 images from PASCAL VOC datasets (explanation in Sec. 4.6).

Methods	Train	Batch	Sup.	Time
CoreSet [49]	✓	✓	✓	~ 42 hours + label query
Learn Loss [61]	✓	✓	✓	
MC-dropout [20]	✓	✓	✓	
CDAL-CS [1]	✓	✓	✓	
VAAL [52]	✓	✓	✗	~ 42 hours
GEAL (ours)	✗	✗	✗	648 seconds

baselines. When compared with existing active learning methods following the traditional pipeline, our algorithm can still achieve *competitive or even better performance* in addition to significantly advantageous generality and efficiency. Besides, our algorithm is very *simple* and *intuitive* with only hours of efforts for implementation.

Our main contributions are summarized as follows.

- We propose a novel pipeline for active learning by discarding the model training and batch selection on each dataset. The pipeline follows the principle of *generality*, *efficiency*, and *non-supervision*.
- We design a novel active learning algorithm, GEAL, following the new pipeline. It selects samples based on our newly defined *knowledge clusters* extracted from intermediate features.
- Our algorithm achieves impressive performances on different tasks over various datasets. It verifies the effectiveness of the proposed pipeline and algorithm, taking a solid step towards general and efficient active learning.

2. Related Work

Active learning Active learning aims to choose the most suitable samples for annotation from a large unlabeled dataset so that model performances can be optimized with a limited annotation budget. Previous work can be divided into three categories: *query-synthesizing methods*, *stream-based methods* and *pool-based methods*. *Query-synthesizing methods* [39, 40, 65] synthesize samples based on the request of learners with a *generative model*. This model is often difficult to train and highly specific to data domains. *Stream-based methods* make a judgment on whether each sample should be labeled independently,

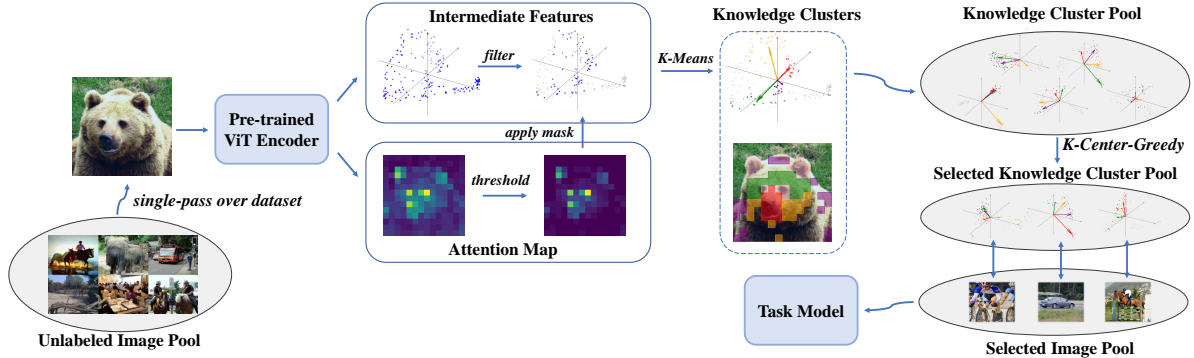


Figure 2. **Overview of our proposed GEAL:** Our method relies on a general pre-trained vision transformer to extract features from images. Knowledge clusters are derived from the intermediate features. Afterwards, we perform K -Center-Greedy algorithm to select knowledge clusters as well as the associated images. These selected images are labeled for downstream task model training.

which allows them to deal with sequential samples online. However, these methods usually require either a large dataset to train the selection policy [18, 57] or an online annotator to update the decision model [41, 42], both of which are unavailable in many cases.

Due to the difficulties of other two categories, most existing arts [25, 43, 49, 52, 61, 62] follow the *pool-based* protocol. Unlike *stream-based methods*, it selects samples based on the ranking of the whole dataset. There exist two mainstream sampling strategies for pool-based methods *i.e.* *uncertainty* and *diversity*. Uncertainty inside the model prediction reflects the difficulty of data samples, which is estimated with different heuristics such as probabilistic models [15, 23], entropy [29, 37], ensembles [2, 34], and distance from decision boundary [3, 54]. Unfortunately, most uncertainty-based methods cannot fit large datasets and deep models well [49]. Alternatively, some other algorithms [1, 28, 49] try to find the most *diverse* subset which well represents the entire dataset. Sener and Savarese [49] theoretically prove that data selection is equivalent with k -Center problem [19] *i.e.* minimizing the maximal distance between data points and selected samples. They implement it with Euclidean distance between high-dimensional features, which is challenged by [52] and [1]. Instead, Sinha et al. [52] train a Variational Autoencoder (VAE) to represent the input, while Agarwal et al. [1] apply the KL -divergence between local region representations. However, all these methods, including some combinations of *uncertainty* and *diversity* [31, 56], rely on a small initial set to learn the deep models for feature extraction, which is insufficient to support a successful training process. As a compromise, they have to repetitively select data in batch, and train the model *multiple times*, significantly degrading the efficiency.

Different from all these active learning methods above, we propose a different pipeline. We directly borrow an accessible pre-trained model, and select samples on *any* datasets through a *single-pass inference*.

Unsupervised representation learning Currently, contrastive methods [7, 24, 26, 45, 53, 58, 63] have achieved great success in unsupervised representation learning, where models are trained to discriminate different images without using any explicit categories. Some early work [7, 8, 26, 59] implement it by reducing the distances between representations from views of the same image (positive pairs) while splitting apart the representations from views of different images (negative pairs). By updating the parameters with moving average, Grill et al. [24] successfully eliminate the negative pairs. Such a strategy inspires many following approaches [32, 60]. Recently, [4] and [9] explore the self-supervised learning of vision transformer (ViT) [14], where [4] also shows that self-attention map serve as a great indicator of region importance.

In this paper, we use the pre-trained model [4] to extract features on different datasets. As a result, we do not have to train deep models separately for each dataset as did in the traditional pipeline, ensuring the generality of our method.

3. Methods

In this section, we will introduce our novel active learning method GEAL in detail. Firstly, in Sec. 3.1, we show that trivial utilization of off-the-shelf global features extracted by a pre-trained model fails in active learning. It spurs the necessity of designing a novel general and efficient active learning method. Then, we define a new notion called *knowledge cluster* in Sec. 3.2, which is important for GEAL. Afterwards, we further elaborate the sample selection strategy in Sec. 3.3. An overview of our approach is illustrated in Fig. 2.

3.1. Off-the-Shelf Features for Active Learning

Previous work in the field of active learning [1, 49, 52] typically selects representative samples based on the features extracted by deep models. These deep models are trained separately over each dataset. Here we take a step

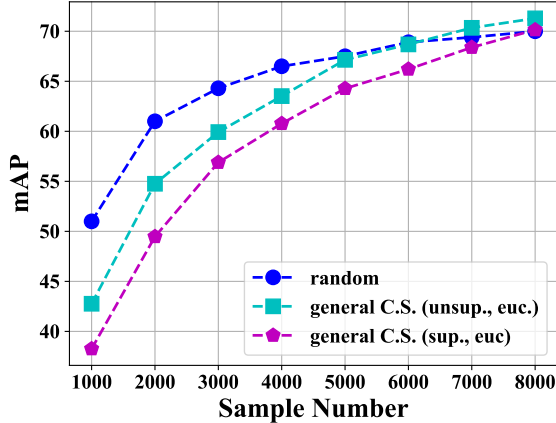


Figure 3. **Preliminary: Core-Set over off-the-shelf Global Features:** *C.S.* denotes Core-Set in this figure. We directly perform Core-Set algorithm over off-the-shelf global features extracted by ViT-Small model pre-trained on ImageNet dataset. We follow [49] to use euclidean distance (*euc.*). This setting causes a significant performance drop, especially when sample number is small.

back and try to use off-the-shelf features instead, which are extracted by general models pre-trained on a large-scale dataset. If it performs well, we can significantly improve the generality and efficiency of active learning by eliminating the model training step.

We conduct this experiment on object detection task over PASCAL VOC dataset [17] with SSD-300 model [36]. Consistent with our following experiments, we apply ViT-Small [55] model¹ for feature extraction in the data selection process. The model is pre-trained in either supervised or unsupervised (with DINO framework [4]) manner on ImageNet dataset [13]. For active learning, we directly implement a classical Core-Set algorithm [49] by running *K-Center-Greedy* over class token outputs. This algorithm selects different percentages of training data, and we train object detection models over the selected subsets.

In Fig. 3, we show results in comparison with random selection. Unfortunately, we find that active learning over off-the-shelf global features degrades the performance of object detection task model, especially with relatively few samples. We consider two potential reasons for this failure:

- **Complex scenes are hard to represent globally.** Images in PASCAL VOC dataset usually contain multiple objects, and object detection tasks rely on local information in a great extent. Thus, it is difficult for a global feature to represent all the useful details in an image.
- **K-Center-Greedy tends to select simple scenes.** Global features of simple images are easily distant from each other if they contain distinct instances. In

contrast, if there are multiple instances in complex images, information inside them is more likely to overlap with each other. As a result, the farthest-distance-based selection prefers to select the simple images with few instances, which damages the training of object detection models.

The above two concerns inspire our design of new active learning methods. We represent each image with dense features instead of a single global feature so that useful local information is not ignored. Also, images are selected based on the distance between *knowledge clusters* instead of global features, which relieves the harmful preference for simple images.

3.2. Knowledge Clusters inside Images

To represent useful local visual cues, we pay attention to intermediate features of neural networks. We consider the feature of the i -th intermediate layer for image I as $I\mathbf{f}_i = \{I f_i^r \in \mathbb{R}^{K_i} | r = 1, 2, \dots, H_i W_i\}$. Here K_i is the feature dimension, while H_i, W_i are the height and width of the feature map in layer i . $I f_i^r \in \mathbb{R}^{K_i}$ is defined as the feature corresponding to region r in the feature map. For simplicity, we write $I\mathbf{f}_i, I f_i^r$ as \mathbf{f}_i, f_i^r for image I without ambiguity. In a deep layer, it reflects the discriminative power of visual patterns inside the region r . This makes sense in both convolutional neural networks [33] and vision transformers [46].

However, it still remains challenging to extract *reliable* local information directly from \mathbf{f}_i due to the following two concerns. (i) Given the low information density inside images, many regions are useless or even distracting for downstream tasks. (ii) Local features extracted by DNNs inevitably contain noise, *i.e.*

$$f_i^r = \hat{f}_i^r + \epsilon_i^r \quad (1)$$

where \hat{f}_i^r is the clean feature, and $\epsilon_i^r \in \mathcal{N}(\mathbf{0}, I_{K_i})$ is noise.

For the first concern, the *class token* self-attention map of the transformer can serve as a natural indicator of regional importance even without dense supervision [4]. For the i -th layer of image I , the self-attention map is denoted as $I\mathbf{attn}_i = \{I\text{attn}_i^r \in \mathbb{R}^+ | r = 1, \dots, H_i W_i\}$, $\sum_{r=1}^{H_i W_i} I\text{attn}_i^r = 1$. We also write $I\mathbf{attn}_i, I\text{attn}_i^r$ of image I as $\mathbf{attn}_i, \text{attn}_i^r$ for simplicity. Since features in deep layers have stronger discriminative power [33], we obtain useful local features based on the last layer attention \mathbf{attn}_n ² of ViT encoder [14, 55]. To be specific, we can distill the important regional features that jointly represent most information in the entire image, as

¹We follow the name in [4]. ViT-Small model is exactly DeiT-S in [55] without the distillation token.

²Notice that the attention in the last layer is computed over the intermediate-features in the second last layer

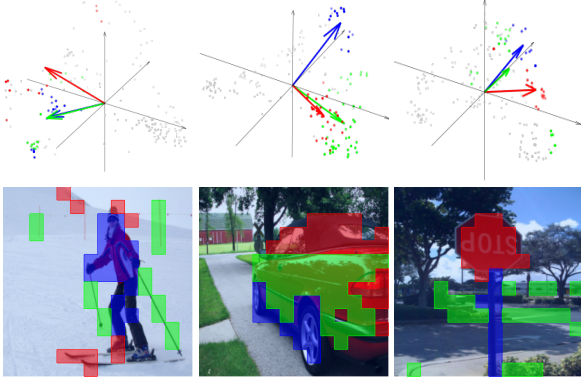


Figure 4. **Visualization of Knowledge Clusters:** *Top:* The distilled intermediate features of each image are grouped into different knowledge clusters. Gray features are eliminated in Eq. 2. Dimensions are reduced through PCA for visualization. *Bottom:* Regions inside images can be associated with corresponding knowledge clusters.

shown in Eq. 2.

$$F(\mathbf{f}_{n-1}) = \{f_{n-1}^r | r = 1, \dots, t, \sum_{j=1}^t \text{attn}_n^j \leq \tau < \sum_{j=1}^{t+1} \text{attn}_n^j\} \quad (2)$$

where the regions $r = 1, \dots, H_i W_i$ are sorted in the decreasing order of attn_n^r , and $\tau \in (0, 1)$ is a hyper-parameter, meaning the maintained ratio of information represented by the distilled important features.

For the second concern, to eliminate the noise, we perform *K-Means* clustering over the distilled intermediate features $F(\mathbf{f}_{n-1})$ to get K centroids ${}^I\mathbf{c} = \{{}^I c_j | j = 1, \dots, K\}$, where K is a hyper-parameter. In this case, we can derive Eq. 3. The noise can be counteracted if it approximately obeys the Gaussian distribution.

$$\begin{aligned} {}^I c_j &= \frac{1}{|C_j|} \sum_{r \in C_j} f_{n-1}^r \\ &= \frac{1}{|C_j|} \sum_{r \in C_j} \hat{f}_{n-1}^r + \frac{1}{|C_j|} \sum_{r \in C_j} \epsilon_{n-1}^r \\ &\approx \frac{1}{|C_j|} \sum_{r \in C_j} \hat{f}_{n-1}^r \end{aligned} \quad (3)$$

where $f_{n-1}^r \in F(\mathbf{f}_{n-1})$, $r \in C_j$ are distilled features of image I grouped into cluster j . Here ${}^I c_j, j = 1, 2, \dots, K$ are defined as *knowledge clusters* inside the image I . We visualize some examples in Fig. 4.

3.3. Sample Selection Strategy for GEAL

Our main target of data selection is to make the distributions of selected data as close to the entire dataset as possible in the level of *knowledge clusters* instead of images.

This fine-grained strategy guarantees that our selected subset can cover as diverse as possible local visual patterns, which are crucial for detection and segmentation tasks.

Inspired by [49], we transplant their theoretically grounded idea of Core-Set to the *knowledge cluster* level. That is to say, we try to minimize the radius δ of $\mathbb{R}^{K_{n-1}}$ -balls around each selected knowledge cluster, whose union covers all the *knowledge clusters* contained in the entire dataset. The detailed algorithm is shown in Alg. 1. In concise, we apply a *K-Center-Greedy* algorithm w.r.t. *knowledge clusters*. Given an unlabeled image pool \mathcal{I} , this process starts from randomly selecting an initial image I_0 i.e. selecting all knowledge clusters ${}^{I_0}\mathbf{c}$ inside it. Then, we choose the image I that contains the knowledge cluster ${}^I c_j$ farthest from already selected clusters (Eq. 4).

$$I, j = \underset{j=1, \dots, K}{\operatorname{argmax}} \min_{c \in s_{\mathcal{K}}} d({}^I c_j, c) \quad (4)$$

where $s_{\mathcal{K}}$ is the pool of all already selected knowledge clusters. When we choose an image I , all the knowledge clusters ${}^I c_j$ inside it are put into the selected pool. This process continues until enough images have been selected. It is worth noting that the selection only relies on the features extracted offline beforehand. Consequently, only *single-pass* model inference *without* any training or supervision is required in the entire active learning pipeline.

Algorithm 1: Data Selection Algorithm

Input: all knowledge clusters \mathbf{c} , total annotation budget b

Output: selected image pool $s_{\mathcal{I}}$

- 1 Initialize $s_{\mathcal{I}} = \{I_0\}$
 - /* initialize the selected image pool with a random image I_0 */
- 2 Initialize $s_{\mathcal{K}} = \{{}^{I_0} c_j, j = 1, \dots, K\}$
 - /* initialize the selected knowledge cluster pool with knowledge clusters inside I_0 */
- 3 repeat
- 4 $I, j = \underset{j=1, \dots, K}{\operatorname{argmax}} \min_{c \in s_{\mathcal{K}}} d({}^I c_j, c)$
 - /* find knowledge cluster ${}^I c_j$ farthest from currently selected ones */
- 5 $s_{\mathcal{I}} = s_{\mathcal{I}} \cup \{I\}$
 - /* add image I to selected image pool */
- 6 $s_{\mathcal{K}} = s_{\mathcal{K}} \cup \{{}^I c_j, j = 1, \dots, K\}$
 - /* add all knowledge clusters in image I to selected knowledge cluster pool */
- 7 until $|s_{\mathcal{I}}| = b$

4. Experiments

In this section, we evaluate our proposed GEAL on the tasks of object detection (Sec. 4.2), image classification

(Sec. 4.3), semantic segmentation (Sec. 4.4), and depth estimation (Sec. 4.5). The results of GEAL are *averaged* over *three* independent selections with different random seeds. Image features in different datasets are extracted by the same general pre-trained model (Sec. 4.1). Then we make some analysis in Sec. 4.6. Finally, we examine the sensitivity of the proposed method to some hyper-parameters in Sec. 4.7. We refer readers to the *supplementary materials* for more implementation details and analysis.

4.1. General Model for Feature Extraction

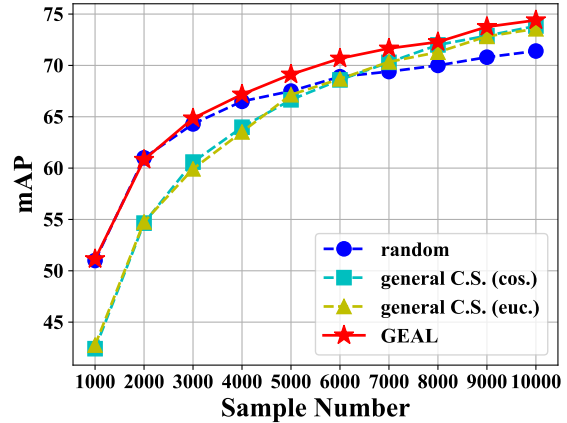
We adopt ViT-Small [55] model (path size 16×16) pre-trained with the unsupervised framework DINO [4] on ImageNet dataset [13] to extract features for data selection due to its great performance and compatibility. The same pre-trained model is used for all tasks. For each image I in various datasets, knowledge clusters I_c are derived based on the last layer class token self-attention I_{attn_n} (average of multi-heads) and second last layer features $I_{f_{n-1}}$ (Sec. 3.2).

4.2. Object Detection

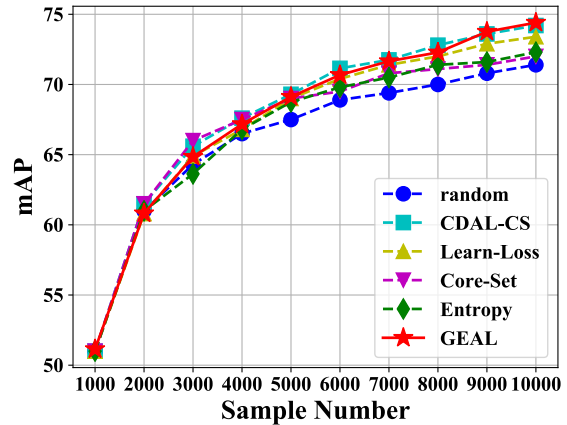
Dataset and Task Model We carry out experiments on PASCAL VOC dataset [17]. Following prior work [1, 61], we combine the training and validation sets of PASCAL VOC 2007 and 2012 as the unlabeled training pool with 16,551 images. The performance of task model is evaluated on PASCAL VOC 2007 test set using mAP metric. For fairness of comparison, we follow previous work [1, 61] to use SSD-300 model [36] with VGG-16 backbone [51], which would be trained on the selected samples. This model reaches 77.43 mAP with 100% training data.

Results In Fig. 5a, we demonstrate the performance of GEAL. Besides random selection, we also compare our methods with two baselines, which directly perform Core-Set algorithm with *cosine* and *euclidean* distances over the global features extracted with the same pre-trained ViT-Small model. It is easy to see that only our GEAL performs well in all sample ratios, while the other two baselines fail when the sample number is small.

Comparison with Traditional Pipeline Methods We compare the performance of GEAL with state-of-the-art methods following traditional pipeline in Fig. 5b. Despite following the new pipeline, GEAL can still be classified as a pool-based method compatible with multiple tasks. Thus we mainly compare it with other task-agnostic pool-based work. Our performance is better than most of them, and remains competitive with the best one (*i.e.* CDAL-CS [1]). It is worth emphasizing that these previous methods require repetitive model training and data selection on each dataset separately so that our method is significantly superior to all of them in generality and efficiency.



(a) Comparison with Random Selection and General Baselines: C.S. means Core-Set, while *cos.* and *euc.* separately denote *cosine* and *euclidean* distance function. Our method has notable superiority in all cases.



(b) Comparison with Traditional Pipeline Methods: With significant advantage on generality and efficiency, our method is also equipped with a advanced performance competitive with or better than approaches following the traditional pipeline.

Figure 5. Active Learning Performance on Object Detection: The mAP on 100% training data is 77.43.

4.3. Image Classification

Dataset and Task Model Since knowledge clusters are extracted based on dense intermediate features, GEAL is more suitable for images with large size. Therefore, instead of CIFAR dataset [30] (32×32 image size), we use Oxford-IIIT Pet dataset [44] for the image classification experiment. It includes 37 pet categories with roughly 200 images for each class. We report the result using *Top-1 Accuracy* metric. ResNet-50 classification model [27] is used in this task. The model reaches 93.13% Top-1 Accuracy with 100% training data.

Results We demonstrate the results of active learning in Fig. 6. Same as object detection task, we compare our GEAL with two baselines: *general Core-Set (cos.)* and *gen-*

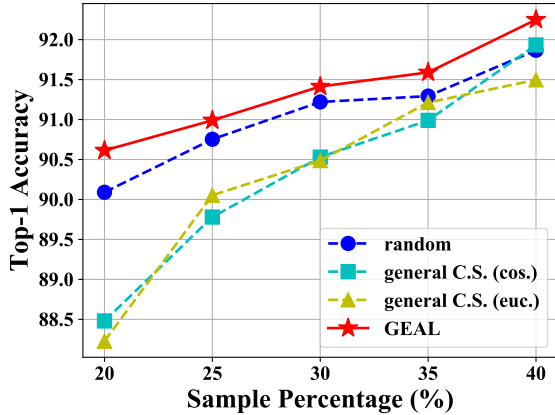


Figure 6. **Active Learning Performance on Image Classification Task:** C.S. means Core-Set. The Top-1 Accuracy on 100% training data is 93.13%.

eral Core-Set (euc.) as well as random selection. Although image classification is more related to global features, to our surprise, the other two baselines still perform much worse than random selection. In contrast, our design of GEAL is also successful for image classification.

4.4. Semantic Segmentation

Dataset and Task Model We use Cityscapes [12] dataset for semantic segmentation, which is composed of 3,475 frames with pixel-level annotation of 19 object classes. We report the result using *mIoU* metric. DeepLabV3 model [6] with ResNet-18 backbone [27] is adopted for this task. This model reaches 76.60 mIoU with 100% training data.

Results We compare GEAL with random selection. Since there is a notable domain gap between the pre-training dataset (*i.e.* ImageNet) and Cityscapes, it is quite challenging to apply the general active learning method. However, based on results in Fig. 7, GEAL still brings solid improvement in comparison with random selection.

4.5. Depth Estimation

Dataset and Task Model We use the KITTI 2015 stereo dataset [21] with the data split in [16] for depth estimation. We follow [22, 64] to remove static frames. There remain 39,810 monocular triplets for training and 4,424 for validation. Results are reported using *Abs Rel* metric. The lower *Abs Rel* is better. We apply Monodepth2 [22] model with ResNet-18 backbone [27]. The model trained from scratch reaches 0.132 *Abs Rel* with 100% training data.

Results The active learning performance on depth estimation is visualized in Fig. 8. Similar to Cityscapes, the domain gap between KITTI and ImageNet is also signifi-

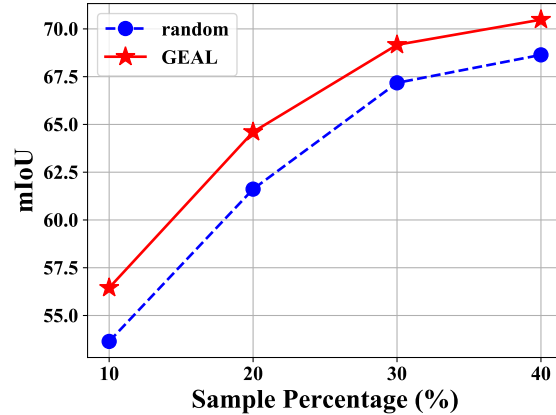


Figure 7. **Active Learning Performance on Semantic Segmentation Task:** The mIoU on 100% training data is 76.60.

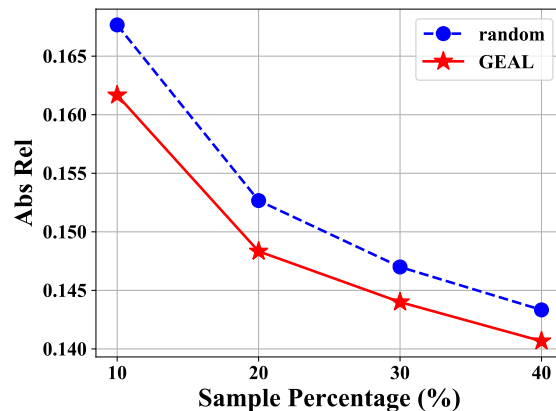


Figure 8. **Active Learning Performance on Depth Estimation Task:** The *Abs Rel* reaches 0.132 with 100% training data. Lower *Abs Rel* is better.

cant. However, our method could still achieve notable performance gain on this task.

4.6. Analysis

Instance Number We count the sum of instance numbers inside selected images of PASCAL VOC in Fig. 9. Interestingly, although GEAL achieves much better performance than random selection, fewer instances lie in the images chosen by GEAL. This counter-intuitive fact reveals that GEAL could find the most informative and diverse high-quality instances even without supervision. For one thing, it further decreases the labor and expense of annotation. For another, this phenomenon motivates us to rethink the correlation between model performance and annotation quantity.

Time Efficiency Analysis Time efficiency of active learning methods is crucial for its practical use. Tab. 1 shows the comparison between GEAL and other existing counterparts. The experiment and estimation are conducted over

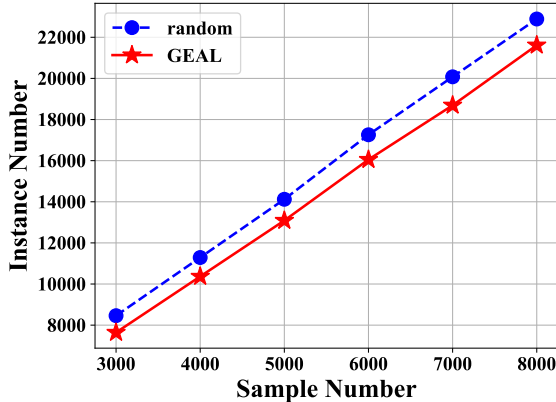


Figure 9. **Number of Instances inside Selected Images** The number is counted on PASCAL VOC dataset. GEAL selects fewer instances than random selection when the image number is same.

PASCAL VOC dataset where 8,000 samples are chosen. We follow their papers [1, 49, 52] to use VGG-16 backbone for previous methods, and the task model for object detection is SSD-300 (same as Sec. 4.2). The time is estimated on a single NVIDIA TITAN RTX GPU. For our GEAL, since it directly utilizes the public pre-trained model *instead of* training models separately for each dataset, only the feature extraction, knowledge cluster construction, and data selection time should be considered, *i.e.* 648 seconds in total. In contrast, for other work following the traditional pipeline, networks are trained repetitively on each dataset. Compared to the training, their model inference and data selection time can be ignored for convenience. We follow [1, 61] to set their initial set size and batch selection budget both as $1k$. For Core-Set [49], Learn Loss [61], VAAL [52], MC-dropout [20], and CDAL-CS [1], their model should be trained for 7 times on subset of size $1k \sim 7k$. Due to the special network architectures of VAAL and Learn Loss, they need more training time than standard object detectors. For convenience, we optimistically estimate their training efficiency the same as object detector SSD-300, which requires about 42 hours in total. For the above methods except VAAL, they also need to wait the oracle for ground-truth labels after each batch selection. Based on the above information, our method is about **233x** faster than prior work.

4.7. Ablation Study

We shed light on the effect of some hyper-parameters including attention ratio τ (Sec. 3.2), centroid number K (Sec. 3.2) and distance function $d(\cdot, \cdot)$ (Sec. 3.3). The experiments are conducted on PASCAL VOC dataset with the same settings in Sec. 4.2. The results are shown in Tab. 2. We refer readers to more ablation studies in Sec. B.

Table 2. **Ablation Study:** τ , K , $d(\cdot, \cdot)$ separately denote the attention ratio, centroid number, and distance function.

τ	K	$d(\cdot, \cdot)$	Sample Number		
			$3k$	$5k$	$7k$
0.4	25	cos.	64.18	68.61	71.02
0.5			64.85	69.12	71.66
0.6			64.19	69.07	71.87
0.5	5	cos.	64.62	69.00	71.74
	15		64.36	68.95	71.68
0.5	25	euc.	63.70	68.70	71.76

Attention Ratio Experiments verify the benefit of a moderate threshold, which serves as a trade-off between information completeness and noise elimination. We also find higher threshold works better if more images are selected. It may be explained that more samples can allow for more noise in some of the selected images.

Centroid Number From the results, our method is not very sensitive to the centroid number. In most situations, more centroids would bring better performance. In this case, features in the same cluster become similar, which allows them to accurately represent the local visual patterns.

Distance Function Different from [49], we find *cosine* distance usually works better than *euclidean*. It agrees with [33] that the intermediate features can be modelled with von Mises-Fisher (vMF) mixture model.

5. Conclusion and Limitations

In this paper, we proposed a novel general, efficient, and unsupervised active learning method GEAL. Challenging the necessity of repetitively training models for each dataset, we extracted features with a general unsupervised pre-trained model. Through a single-pass model inference, the knowledge clusters were derived based on the intermediate features, over which *K-Center-Greedy* algorithm was performed to find the most diverse and informative data samples. We demonstrated promising results on different tasks including object detection, image classification, semantic segmentation, and depth estimation.

We also realized that GEAL cannot outperform all the pool-based approaches following the traditional pipeline now. To this end, we will continue to polish this method with the new pipeline in the future. Nevertheless, this direction is still worth exploring due to its superior generality and efficiency. We believe this paper takes the important and solid first step, and it would inspire further work towards general and efficient active learning.

References

- [1] Sharat Agarwal, Himanshu Arora, Saket Anand, and Chetan Arora. Contextual diversity for active learning. In *European Conference on Computer Vision*, pages 137–153. Springer, 2020. [2](#), [3](#), [6](#), [8](#), [12](#), [13](#)
- [2] William H Beluch, Tim Genewein, Andreas Nürnberger, and Jan M Köhler. The power of ensembles for active learning in image classification. In *Proceedings of the IEEE Conference on Computer Vision and Pattern Recognition*, pages 9368–9377, 2018. [3](#)
- [3] Klaus Brinker. Incorporating diversity in active learning with support vector machines. In *Proceedings of the 20th international conference on machine learning (ICML-03)*, pages 59–66, 2003. [3](#)
- [4] Mathilde Caron, Hugo Touvron, Ishan Misra, Hervé Jégou, Julien Mairal, Piotr Bojanowski, and Armand Joulin. Emerging properties in self-supervised vision transformers. *arXiv preprint arXiv:2104.14294*, 2021. [2](#), [3](#), [4](#), [6](#), [12](#)
- [5] Kai Chen, Jiaqi Wang, Jiangmiao Pang, Yuhang Cao, Yu Xiong, Xiaoxiao Li, Shuyang Sun, Wansen Feng, Ziwei Liu, Jiarui Xu, Zheng Zhang, Dazhi Cheng, Chenchen Zhu, Tianheng Cheng, Qijie Zhao, Buyu Li, Xin Lu, Rui Zhu, Yue Wu, Jifeng Dai, Jingdong Wang, Jianping Shi, Wanli Ouyang, Chen Change Loy, and Dahua Lin. MMDetection: Open mmlab detection toolbox and benchmark. *arXiv preprint arXiv:1906.07155*, 2019. [13](#)
- [6] Liang-Chieh Chen, George Papandreou, Florian Schroff, and Hartwig Adam. Rethinking atrous convolution for semantic image segmentation. *arXiv preprint arXiv:1706.05587*, 2017. [7](#), [13](#)
- [7] Ting Chen, Simon Kornblith, Mohammad Norouzi, and Geoffrey Hinton. A simple framework for contrastive learning of visual representations. In *International conference on machine learning*, pages 1597–1607. PMLR, 2020. [3](#)
- [8] Xinlei Chen, Haoqi Fan, Ross Girshick, and Kaiming He. Improved baselines with momentum contrastive learning. *arXiv preprint arXiv:2003.04297*, 2020. [3](#)
- [9] Xinlei Chen, Saining Xie, and Kaiming He. An empirical study of training self-supervised vision transformers. *arXiv preprint arXiv:2104.02057*, 2021. [3](#)
- [10] MMSegmentation Contributors. MMSegmentation: Openmmlab semantic segmentation toolbox and benchmark. <https://github.com/open-mmlab/mms Segmentation>, 2020. [13](#)
- [11] MMClassification Contributors. Openmmlab’s image classification toolbox and benchmark. <https://github.com/open-mmlab/mmclassification>, 2020. [14](#)
- [12] Marius Cordts, Mohamed Omran, Sebastian Ramos, Timo Rehfeld, Markus Enzweiler, Rodrigo Benenson, Uwe Franke, Stefan Roth, and Bernt Schiele. The cityscapes dataset for semantic urban scene understanding. In *Proceedings of the IEEE conference on computer vision and pattern recognition*, pages 3213–3223, 2016. [7](#)
- [13] Jia Deng, Wei Dong, Richard Socher, Li-Jia Li, Kai Li, and Li Fei-Fei. Imagenet: A large-scale hierarchical image database. In *2009 IEEE conference on computer vision and pattern recognition*, pages 248–255. Ieee, 2009. [1](#), [2](#), [4](#), [6](#)
- [14] Alexey Dosovitskiy, Lucas Beyer, Alexander Kolesnikov, Dirk Weissenborn, Xiaohua Zhai, Thomas Unterthiner, Mostafa Dehghani, Matthias Minderer, Georg Heigold, Sylvain Gelly, et al. An image is worth 16x16 words: Transformers for image recognition at scale. *arXiv preprint arXiv:2010.11929*, 2020. [3](#), [4](#)
- [15] Sayna Ebrahimi, Mohamed Elhoseiny, Trevor Darrell, and Marcus Rohrbach. Uncertainty-guided continual learning with bayesian neural networks. *arXiv preprint arXiv:1906.02425*, 2019. [3](#)
- [16] David Eigen and Rob Fergus. Predicting depth, surface normals and semantic labels with a common multi-scale convolutional architecture. In *Proceedings of the IEEE international conference on computer vision*, pages 2650–2658, 2015. [7](#)
- [17] Mark Everingham, Luc Van Gool, Christopher KI Williams, John Winn, and Andrew Zisserman. The pascal visual object classes (voc) challenge. *International journal of computer vision*, 88(2):303–338, 2010. [2](#), [4](#), [6](#), [12](#)
- [18] Meng Fang, Yuan Li, and Trevor Cohn. Learning how to active learn: A deep reinforcement learning approach. *arXiv preprint arXiv:1708.02383*, 2017. [3](#)
- [19] Reza Zanfirani Farahani and Masoud Hekmatfar. *Facility location: concepts, models, algorithms and case studies*. Springer Science & Business Media, 2009. [3](#)
- [20] Yarin Gal and Zoubin Ghahramani. Dropout as a bayesian approximation: Representing model uncertainty in deep learning. In *international conference on machine learning*, pages 1050–1059. PMLR, 2016. [2](#), [8](#)
- [21] Andreas Geiger, Philip Lenz, and Raquel Urtasun. Are we ready for autonomous driving? the kitti vision benchmark suite. In *2012 IEEE conference on computer vision and pattern recognition*, pages 3354–3361. IEEE, 2012. [7](#)
- [22] Clément Godard, Oisín Mac Aodha, Michael Firman, and Gabriel J Brostow. Digging into self-supervised monocular depth estimation. In *Proceedings of the IEEE/CVF International Conference on Computer Vision*, pages 3828–3838, 2019. [7](#), [13](#)
- [23] Marc Gorriz, Axel Carlier, Emmanuel Faure, and Xavier Giro-i Nieto. Cost-effective active learning for melanoma segmentation. *arXiv preprint arXiv:1711.09168*, 2017. [3](#)
- [24] Jean-Bastien Grill, Florian Strub, Florent Altché, Corentin Tallec, Pierre H Richemond, Elena Buchatskaya, Carl Doersch, Bernardo Avila Pires, Zhaohan Daniel Guo, Mohammad Gheshlaghi Azar, et al. Bootstrap your own latent: A new approach to self-supervised learning. *arXiv preprint arXiv:2006.07733*, 2020. [3](#)
- [25] Elmar Haussmann, Michele Fenzi, Kashyap Chitta, Jan Ivanek, Hanson Xu, Donna Roy, Akshita Mittel, Nicolas Koumchatzky, Clement Farabet, and Jose M Alvarez. Scalable active learning for object detection. In *2020 IEEE Intelligent Vehicles Symposium (IV)*, pages 1430–1435. IEEE, 2020. [3](#)
- [26] Kaiming He, Haoqi Fan, Yuxin Wu, Saining Xie, and Ross Girshick. Momentum contrast for unsupervised visual representation learning. In *Proceedings of the IEEE/CVF Conference on Computer Vision and Pattern Recognition*, pages 9729–9738, 2020. [3](#)

- [27] Kaiming He, Xiangyu Zhang, Shaoqing Ren, and Jian Sun. Deep residual learning for image recognition. In *Proceedings of the IEEE conference on computer vision and pattern recognition*, pages 770–778, 2016. [6](#), [7](#), [13](#), [14](#)
- [28] Suyog Dutt Jain and Kristen Grauman. Active image segmentation propagation. In *Proceedings of the IEEE Conference on Computer Vision and Pattern Recognition*, pages 2864–2873, 2016. [3](#)
- [29] Ajay J Joshi, Fatih Porikli, and Nikolaos Papanikolopoulos. Multi-class active learning for image classification. In *2009 IEEE Conference on Computer Vision and Pattern Recognition*, pages 2372–2379. IEEE, 2009. [3](#)
- [30] Alex Krizhevsky, Geoffrey Hinton, et al. Learning multiple layers of features from tiny images. 2009. [6](#)
- [31] Weicheng Kuo, Christian Häne, Esther Yuh, Pratik Mukherjee, and Jitendra Malik. Cost-sensitive active learning for intracranial hemorrhage detection. In *International Conference on Medical Image Computing and Computer-Assisted Intervention*, pages 715–723. Springer, 2018. [3](#)
- [32] Junnan Li, Pan Zhou, Caiming Xiong, and Steven CH Hoi. Prototypical contrastive learning of unsupervised representations. *arXiv preprint arXiv:2005.04966*, 2020. [3](#)
- [33] Mingjie Li, Shaobo Wang, and Quanshi Zhang. Visualizing the emergence of intermediate visual patterns in dnns. *arXiv preprint arXiv:2111.03505*, 2021. [4](#), [8](#)
- [34] Xin Li and Yuhong Guo. Adaptive active learning for image classification. In *Proceedings of the IEEE Conference on Computer Vision and Pattern Recognition*, pages 859–866, 2013. [3](#)
- [35] Hubert Lin, Paul Upchurch, and Kavita Bala. Block annotation: Better image annotation with sub-image decomposition. In *Proceedings of the IEEE/CVF International Conference on Computer Vision*, pages 5290–5300, 2019. [1](#)
- [36] Wei Liu, Dragomir Anguelov, Dumitru Erhan, Christian Szegedy, Scott Reed, Cheng-Yang Fu, and Alexander C Berg. Ssd: Single shot multibox detector. In *European conference on computer vision*, pages 21–37. Springer, 2016. [4](#), [6](#), [12](#), [13](#)
- [37] David JC MacKay. Information-based objective functions for active data selection. *Neural computation*, 4(4):590–604, 1992. [3](#)
- [38] Dhruv Mahajan, Ross Girshick, Vignesh Ramanathan, Kaiming He, Manohar Paluri, Yixuan Li, Ashwin Bharambe, and Laurens Van Der Maaten. Exploring the limits of weakly supervised pretraining. In *Proceedings of the European conference on computer vision (ECCV)*, pages 181–196, 2018. [1](#)
- [39] Dwarikanath Mahapatra, Behzad Bozorgtabar, Jean-Philippe Thiran, and Mauricio Reyes. Efficient active learning for image classification and segmentation using a sample selection and conditional generative adversarial network. In *International Conference on Medical Image Computing and Computer-Assisted Intervention*, pages 580–588. Springer, 2018. [2](#)
- [40] Christoph Mayer and Radu Timofte. Adversarial sampling for active learning. In *Proceedings of the IEEE/CVF Winter Conference on Applications of Computer Vision*, pages 3071–3079, 2020. [2](#)
- [41] Saad Mohamad, Moamar Sayed-Mouchaweh, and Abdelhamid Bouchachia. Online active learning for human activity recognition from sensory data streams. *Neurocomputing*, 390:341–358, 2020. [3](#)
- [42] Alexander Narr, Rudolph Triebel, and Daniel Cremers. Stream-based active learning for efficient and adaptive classification of 3d objects. In *2016 IEEE International Conference on Robotics and Automation (ICRA)*, pages 227–233. IEEE, 2016. [3](#)
- [43] Hieu T Nguyen and Arnold Smeulders. Active learning using pre-clustering. In *Proceedings of the twenty-first international conference on Machine learning*, page 79, 2004. [3](#)
- [44] Omkar M. Parkhi, Andrea Vedaldi, Andrew Zisserman, and C. V. Jawahar. Cats and dogs. In *IEEE Conference on Computer Vision and Pattern Recognition*, 2012. [6](#)
- [45] Mandela Patrick, Yuki M Asano, Polina Kuznetsova, Ruth Fong, Joao F Henriques, Geoffrey Zweig, and Andrea Vedaldi. Multi-modal self-supervision from generalized data transformations. *arXiv preprint arXiv:2003.04298*, 2020. [3](#)
- [46] Maithra Raghu, Thomas Unterthiner, Simon Kornblith, Chiyuan Zhang, and Alexey Dosovitskiy. Do vision transformers see like convolutional neural networks? In *Thirty-Fifth Conference on Neural Information Processing Systems*, 2021. [4](#)
- [47] Pengzhen Ren, Yun Xiao, Xiaojun Chang, Po-Yao Huang, Zhihui Li, Xiaojiang Chen, and Xin Wang. A survey of deep active learning. *arXiv preprint arXiv:2009.00236*, 2020. [1](#)
- [48] Tal Ridnik, Emanuel Ben-Baruch, Asaf Noy, and Lihi Zelnik-Manor. Imagenet-21k pretraining for the masses. *arXiv preprint arXiv:2104.10972*, 2021. [1](#)
- [49] Ozan Sener and Silvio Savarese. Active learning for convolutional neural networks: A core-set approach. *arXiv preprint arXiv:1708.00489*, 2017. [1](#), [2](#), [3](#), [4](#), [5](#), [8](#)
- [50] Burr Settles. Active learning literature survey. 2009. [1](#)
- [51] Karen Simonyan and Andrew Zisserman. Very deep convolutional networks for large-scale image recognition. *arXiv preprint arXiv:1409.1556*, 2014. [6](#), [13](#)
- [52] Samarth Sinha, Sayna Ebrahimi, and Trevor Darrell. Variational adversarial active learning. In *Proceedings of the IEEE/CVF International Conference on Computer Vision*, pages 5972–5981, 2019. [2](#), [3](#), [8](#), [12](#), [13](#)
- [53] Yonglong Tian, Chen Sun, Ben Poole, Dilip Krishnan, Cordelia Schmid, and Phillip Isola. What makes for good views for contrastive learning? *arXiv preprint arXiv:2005.10243*, 2020. [3](#)
- [54] Simon Tong and Daphne Koller. Support vector machine active learning with applications to text classification. *Journal of machine learning research*, 2(Nov):45–66, 2001. [3](#)
- [55] Hugo Touvron, Matthieu Cord, Matthijs Douze, Francisco Massa, Alexandre Sablayrolles, and Hervé Jégou. Training data-efficient image transformers & distillation through attention. In *International Conference on Machine Learning*, pages 10347–10357. PMLR, 2021. [4](#), [6](#), [12](#), [13](#), [14](#)
- [56] Keze Wang, Dongyu Zhang, Ya Li, Ruimao Zhang, and Liang Lin. Cost-effective active learning for deep image classification. *IEEE Transactions on Circuits and Systems for Video Technology*, 27(12):2591–2600, 2016. [3](#)

- [57] Mark Woodward and Chelsea Finn. Active one-shot learning. *arXiv preprint arXiv:1702.06559*, 2017. [3](#)
- [58] Tete Xiao, Xiaolong Wang, Alexei A Efros, and Trevor Darrell. What should not be contrastive in contrastive learning. *arXiv preprint arXiv:2008.05659*, 2020. [3](#)
- [59] Saining Xie, Jiatao Gu, Demi Guo, Charles R Qi, Leonidas Guibas, and Or Litany. Pointcontrast: Unsupervised pre-training for 3d point cloud understanding. In *European Conference on Computer Vision*, pages 574–591. Springer, 2020. [3](#)
- [60] Zhenda Xie, Yutong Lin, Zheng Zhang, Yue Cao, Stephen Lin, and Han Hu. Propagate yourself: Exploring pixel-level consistency for unsupervised visual representation learning. In *Proceedings of the IEEE/CVF Conference on Computer Vision and Pattern Recognition*, pages 16684–16693, 2021. [3](#)
- [61] Donggeun Yoo and In So Kweon. Learning loss for active learning. In *Proceedings of the IEEE/CVF Conference on Computer Vision and Pattern Recognition*, pages 93–102, 2019. [2](#), [3](#), [6](#), [8](#), [13](#)
- [62] Tianning Yuan, Fang Wan, Mengying Fu, Jianzhuang Liu, Songcen Xu, Xiangyang Ji, and Qixiang Ye. Multiple instance active learning for object detection. In *Proceedings of the IEEE/CVF Conference on Computer Vision and Pattern Recognition*, pages 5330–5339, 2021. [3](#)
- [63] Zaiwei Zhang, Rohit Girdhar, Armand Joulin, and Ishan Misra. Self-supervised pretraining of 3d features on any point-cloud. *arXiv preprint arXiv:2101.02691*, 2021. [3](#)
- [64] Tinghui Zhou, Matthew Brown, Noah Snavely, and David G Lowe. Unsupervised learning of depth and ego-motion from video. In *Proceedings of the IEEE conference on computer vision and pattern recognition*, pages 1851–1858, 2017. [7](#)
- [65] Jia-Jie Zhu and José Bento. Generative adversarial active learning. *arXiv preprint arXiv:1702.07956*, 2017. [2](#)

In this supplementary material, we first give more analysis (Sec. A) and ablation studies (Sec. B), which cannot fit in the *main paper* due to the limited space. In addition, we also provide all the implementation details (Sec. C) to reproduce our results in the experiments.

A. More Analysis

Biased Initialization Prior work [1, 52] following the traditional pipeline often discusses the effect of a biased initial pool. If there is a lack of samples from some categories in the initial pool, the active learning performance would drop significantly, often becoming worse than random selection. However, GEAL is *free from* this problem since we only randomly select *one* initial image and we do *not* train model on the selected images. The effect of initialization is almost negligible *i.e.* the performance is similar no matter which image is randomly sampled initially.

B. More Ablation Studies

In addition to the quantitative studies in Sec. 4.7 of the *main paper*, we give some qualitative insights into the design of GEAL. Same as the *main paper*, we conduct all ablation studies on object detection task over PASCAL VOC [17] dataset with SSD-300 [36] model. The results are shown in Tab. 3.

Feature Map Down-sampling To justify the use of knowledge clusters, we think of some alternative strategies as follows to down-sample the dense feature map.

- A1 Downsizing the intermediate feature map to 5×5 through bilinear interpolation.
- A2 Randomly selecting 25 features from the feature map *without* distilling the important features (Eq. 2 of the *main paper*).
- A3 Randomly selecting 25 features from the feature map *after* distilling the important features (Eq. 2 of the *main paper*).
- A4 Choosing 25 features corresponding to the regions with greatest attention. In this case, the distillation (Eq. 2 of the *main paper*) takes no effect.

Results in Tab. 3 show that all the above alternatives are worse than our proposed knowledge-cluster-based approach, which reflects the superiority of our novel design. We also notice that the performance gaps are not significant when the sample number is large. As far as we are concerned, if there are many images, some bad selections may not greatly affect the training performance. Therefore, alternative down-sampling methods lead to only slightly worse performance when selecting many images.

Distance Reduction In the data selection process, we choose images based on their internal knowledge clusters *farthest* from already selected ones. In this part, inspired by [1], we try an alternative strategy where images are selected based on the *average* distances of internal knowledge clusters so that the selection depends more on the overall condition of the whole image instead of some certain regions. To be specific, Eq. 4 in the *main paper* is replaced with Eq. 5.

$$I = \arg \max_{I \in \mathcal{I}} \frac{1}{K} \sum_{j=1}^K \min_{c \in s_K} d(I c_j, c) \quad (5)$$

This change of reduction manner notably degrades the performance (Tab. 3). We can conclude that key local information is much more important than the overall condition of images in the data selection process for dense supervision tasks such as object detection.

Supervised Pre-training Instead of using the unsupervised framework DINO [4], we attempt the same DeiT-Small model [55] pre-trained in a *supervised* manner on ImageNet. Other settings of active learning remain unchanged. In this case, for many images, most attention is focused on only a few regions. If there are fewer than 25 features in $F(I \mathbf{f}_{n-1})$ after distillation, each of them is directly considered as a separate knowledge cluster without K-Means. According to the results in Tab. 3, the performance drops significantly. We think that the supervised pre-training introduces a strong bias to the pre-trained model. As a result, the model concentrates too much on some details while ignoring other important visual patterns.

C. Implementation Details

In this part, we provide all the detailed pseudo-codes, settings, and hyper-parameters to reproduce our results. The code will also be released after careful arrangement when the paper is accepted.

C.1. Pseudo-Code for Knowledge Cluster Extraction

In this section, we provide the pseudo-code for the first part of GEAL, *i.e.* knowledge cluster extraction (Sec. 3.2 of the *main paper*). The pseudo-code for the second part (*i.e.* data selection) is already shown in Alg. 2 of the *main paper*. Here, given a pre-trained network g and unlabeled image pool \mathcal{I} , we aim to obtain the knowledge clusters $I \mathbf{c}$ for each image $I \in \mathcal{I}$. The detailed algorithm is explained in Alg. 2.

C.2. Object Detection Implementation

Implementation of GEAL We set attention ratio $\tau = 0.5$ and centroid number $K = 25$. The input images are resized

Table 3. **More Ablation Study:** We try different manners for feature map down-sampling, distance reduction, and model pre-training. The last line is our results without any ablations.

Down-sampling	Reduction	Pre-training	Sample Number		
			3k	5k	7k
A1			63.11	68.42	71.28
A2	farthest	DINO	64.11	67.95	71.18
A3			63.78	68.59	71.49
A4			63.76	68.98	71.30
knowledge cluster	average	DINO	62.07	67.56	71.13
knowledge cluster	farthest	supervised	62.86	68.23	70.36
knowledge cluster	farthest	DINO	64.85	69.12	71.66

Algorithm 2: Knowledge Cluster Extraction

Input: pre-trained deep neural network g , unlabeled image pool \mathcal{I} , attention ratio τ , centroid number K

Output: knowledge clusters ${}^I\mathbf{c}$, $I \in \mathcal{I}$

```

1 for  $I \in \mathcal{I}$  do
2    ${}^I\text{attn}_n, {}^I\mathbf{f}_{n-1} = g(I)$ 
   /* extract the last layer attention and
   second last layer intermediate
   features from the network */
   /* only a single-pass model inference is
   required in this process */
3   sort  ${}^I\text{attn}_n^r, {}^I\mathbf{f}_{n-1}^r$ ,  $r = 1, \dots, H_iW_i$  in the
   decreasing order of attention
   /* regions  $r = 1, \dots, H_iW_i$  should be
   arranged in the decreasing order of
    ${}^I\text{attn}_n^r$  */
4    $F({}^I\mathbf{f}_{n-1}) = \{ {}^I\mathbf{f}_{n-1}^r | r = 1, \dots, t,
   \sum_{j=1}^t {}^I\text{attn}_n^j \leq \tau < \sum_{j=1}^{t+1} {}^I\text{attn}_n^j \}$ 
   /* distill important local features
   based on the sorted attention (Eq. 2
   of the main paper) */
5    ${}^I\mathbf{c} = K\text{Means}(F({}^I\mathbf{f}_{n-1}), K)$ 
   /* get  $K$  centroids  ${}^I\mathbf{c}_j, j = 1, \dots, K$  by
   conducting K-Means over  $F({}^I\mathbf{f}_{n-1})$  */

```

to 224×224 when fed into the pre-trained DeiT-Small [55] model.

Implementation of Task Model The SSD-300 model [36] is adopted for this experiment. The model is implemented based on mmdetection [5]. We follow [61] to train the model for 300 epochs with batch size 32 using SGD optimizer (momentum 0.9). The VGG-16 [51] backbone is initialized with ImageNet pre-trained weights. The ini-

tial learning rate is 0.001, which decays to 0.0001 after 240 epochs.

C.3. Semantic Segmentation Implementation

Implementation of GEAL Same as object detection, we set attention ratio $\tau = 0.5$ and centroid number $K = 25$. The input images are resized to 448×224 consistent with their original aspect ratios when fed into the pre-trained DeiT-Small [55] model.

Implementation of Task Model Previous active learning work [1, 52] does not specify their backbones and architectures for semantic segmentation. Consequently, we cannot follow their settings. Instead, we use the classical DeepLabv3 [6] model. The model is implemented based on mmsegmentation [10]. We train the model for $80,000 \cdot s$ iterations with batch size 8, where $s \in (0, 1]$ is the sample ratio, using SGD optimizer (momentum 0.9), as in [10]. The ResNet-18 backbone [27] is initialized with ImageNet pre-trained weights. The learning rate is 0.01 initially and decays in polynomial strategy with power 0.9.

C.4. Depth Estimation Implementation

Implementation of GEAL Same as the previous two tasks, we set attention ratio $\tau = 0.5$ and centroid number $K = 25$. The input images are resized to 640×192 consistent with their original aspect ratios when fed into the pre-trained DeiT-Small [55] model.

Implementation of Task Model We use the MonoDepth2 [22] model with ResNet-18 backbone [27]. We follow their official settings to train the model for 20 epochs with batch-size 12 using Adam optimizer. The model is trained from scratch without any pre-trained weights. The learning rate drops from 10^{-4} to 10^{-5} after 15 epochs.

C.5. Image Classification Implementation

Implementation of GEAL We follow previous tasks to set attention ratio $\tau = 0.5$. Since image classification depends less on local information, we directly set the centroid number $K = 1$. The input images are resized to 224×224 when fed into the pre-trained DeiT-Small [55] model.

Implementation of Task Model We use ResNet-50 [27] classification model in this task, which is implemented based on mmclassification [11]. The model is trained for 80 epochs with batch size 64 using SGD optimizer (momentum 0.9). The backbone is initialized with ImageNet pre-trained weights. The initial learning rate is 0.001 for the classification head and 0.0001 for the backbone. After 60 epochs, the learning rate decays by 10 times.